Separation Science and Technology
Publication details, including instructions for authors and subscription information:
http://www.informaworld.com/smpp/title~content=t713708471

Unsteady-State Permeate Flux of Crossflow Microfiltration: Effect of Particle Size Distribution

Dong-Jang Chang[a]; Shyh-Jye Hwang[a]
[a] DEPARTMENT OF CHEMICAL ENGINEERING, NATIONAL TSING HUA UNIVERSITY, HSINCHU, TAIWAN, REPUBLIC OF CHINA

To cite this Article Chang, Dong-Jang and Hwang, Shyh-Jye(1995) 'Unsteady-State Permeate Flux of Crossflow Microfiltration: Effect of Particle Size Distribution', Separation Science and Technology, 30: 14, 2917 — 2931
To link to this Article: DOI: 10.1080/01496399508013722
URL: http://dx.doi.org/10.1080/01496399508013722

SEPARATION SCIENCE AND TECHNOLOGY, 30(14), pp. 2917–2931, 1995

Unsteady-State Permeate Flux of Crossflow Microfiltration: Effect of Particle Size Distribution

DONG-JANG CHANG and SHYH-JYE HWANG*
DEPARTMENT OF CHEMICAL ENGINEERING
NATIONAL TSING HUA UNIVERSITY
HSINCHU, TAIWAN 30043, REPUBLIC OF CHINA

ABSTRACT

A mathematical model based on a hydrodynamic theory and mass balance was developed for the prediction of the unsteady-state permeate flux in crossflow microfiltration under the influence of particle size distribution. Experiments were also conducted in a membrane filtration cell to verify this model. Spherical polystyrene latex particles of 0.303, 0.606, and 1.020 μm were used to make suspensions of various particle size distributions. The flow of the suspension in the channel of the filtration cell was controlled under the laminar flow region. It was found that the unsteady-state permeate flux increased as the mean particle size of the suspension was increased. Moreover, the model predicted satisfactorily the unsteady-state permeate flux under the effect of particle size distribution.

INTRODUCTION

Crossflow microfiltration provides an excellent alternative to the conventional solid–liquid separation processes. Microparticles, microorganisms, macromolecules, colloids, and most bacteria can be removed effectively by this method. During crossflow microfiltration, the particles in the suspension are continuously pulled toward the membrane surface by the flow of the permeate through the membrane. Simultaneously, the particles are lifted away from the membrane surface by a backtransport force driven by various mechanisms (1–3). When the two counteracting forces

* To whom correspondence should be addressed.

are balanced, a steady-state is reached. At the steady-state the permeate flux and the thickness of the cake on the membrane remain constant.

Many theoretical studies have been made, and several predictive models have been developed to explain the performance of crossflow microfiltration (4–9). Nevertheless, most of the models assumed that the suspension was monodispersed, which did not exist in practical situations. Only a few models have been developed to describe the fouling of crossflow microfiltration for polydispersed suspensions (4, 5). However, the coefficients in those models could not be obtained theoretically.

Chang and Hwang (10) developed a mathematical model based on a hydrodynamic theory and mass balance to predict satisfactorily the unsteady-state permeate flux of crossflow microfiltration for monodispersed suspensions. All of the significant terms of the backtransport force and the hydrodynamic resistances of the membrane and particle layer were considered in their model. For this study their model was modified to predict the unsteady-state permeate flux of crossflow microfiltration for polydispersed suspensions.

THEORETICAL DEVELOPMENT

Hydrodynamic Model

The schematic representation of the model is shown in Fig. 1 (10). The assumptions and derivation of the model are similar to Chang and Hwang

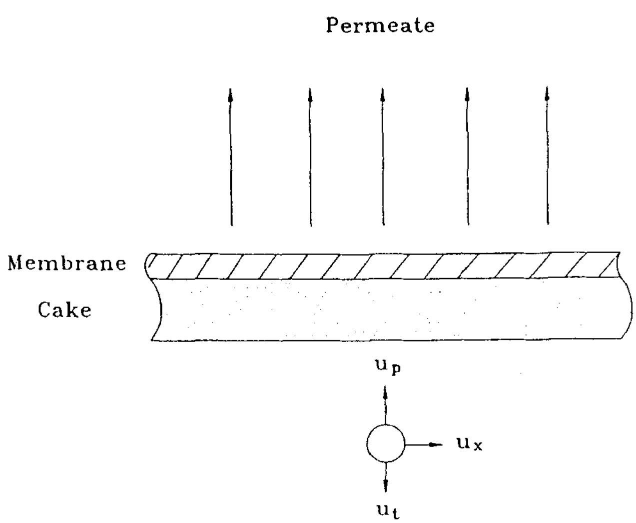

FIG. 1 Schematic representation of the model (10).

(10) except that the cake resistance, R_c, and the permeate flux, u_p, are modified as follows:

$$R_c = \left[\alpha_i\rho_{p1}C_1 \int (u_p - u_{t1}) + \alpha_i\rho_{p2}C_2 \int (u_p - u_{t2}) + \cdots + \alpha_i\rho_{pn}C_n \int (u_p - u_{tn})\right]dt \quad (1)$$

$$u_p = \frac{\Delta P}{\mu\left\{R_m + \left[\alpha_i\rho_{p1}C_1 \int (u_p - u_{t1}) + \alpha_i\rho_{p2}C_2 \int (u_p - u_{t2}) + \cdots + \alpha_i\rho_{pn}C_n \int (u_p - u_{tn})\right]dt\right\}} \quad (2)$$

where R_m is the membrane resistance, ΔP is the pressure drop across the membrane, and α_i is the specific resistance of the instantaneous cake at time t. Integration of Eq. (2) gives

$$\int u_p dt = \frac{(\rho_{p1}C_1u_{t1} + \rho_{p2}C_2u_{t2} + \cdots + \rho_{pn}C_nu_{tn})t}{\rho_{p1}C_1 + \rho_{p2}C_2 + \cdots + \rho_{pn}C_n} + \frac{\Delta P}{\mu\alpha_iu_p(\rho_{p1}C_1 + \rho_{p2}C_2 + \cdots + \rho_{pn}C_n)} - \frac{R_m}{\alpha_i(\rho_{p1}C_1 + \rho_{p2}C_2 + \cdots + \rho_{pn}C_n)} \quad (3)$$

In addition, the crossflow velocity in the filtration channel is

$$u_{oi} = \left[u_o + \frac{(u_{po} - u_{pi})A_m}{A_b}\right]\frac{h}{(h - \sum h_{ci})} \quad (4)$$

where u_o is the crossflow velocity of the suspension measured at the outlet of the filtration cell, and h_{ci} is the instantaneous cake thickness with cake resistance R_{ci}. h_{ci}, the weight of particle size n of the instantaneous cake (W_{ni}), and the mean particle size of the instantaneous cake (d_{pi}), are calculated by

$$h_{ci} = \frac{R_{ci}d_{pi}^2\epsilon_{ci}^3}{180(1 - \epsilon_{ci})^2} \quad (5)$$

$$W_{ni} = \frac{C_{ni}(u_p - u_{tn})\rho_p(1 - \epsilon_{ci})A_m}{C_{1i}(u_p - u_{t1}) + C_{2i}(u_p - u_{t2}) + \cdots + C_{ni}(u_p - u_{tn})} \quad (6)$$

$$d_{\mathrm{pi}} = \frac{\sum N_{\mathrm{i}} d_{\mathrm{p}n}^3}{\sum N_{\mathrm{i}} d_{\mathrm{p}n}^2} = \frac{W_{1\mathrm{i}} + W_{2\mathrm{i}} + \cdots + W_{n\mathrm{i}}}{\frac{W_{1\mathrm{i}}}{d_{\mathrm{p}1}} + \frac{W_{2\mathrm{i}}}{d_{\mathrm{p}2}} + \cdots + \frac{W_{n\mathrm{i}}}{d_{\mathrm{p}n}}} \tag{7}$$

Furthermore, the velocities due to lateral migration, shear-induced diffusion, and Brownian diffusion, and the concentration of each particle size in the suspension should be modified:

$$u_{\mathrm{l}n\mathrm{i}} = \frac{0.43\rho u_{\mathrm{oi}} d_{\mathrm{p}n}^3}{\mu(h - \sum h_{\mathrm{ci}})^2} \tag{8}$$

$$u_{\mathrm{s}n\mathrm{i}} = \frac{u_{\mathrm{oi}} d_{\mathrm{p}n}^2}{20(h - \sum h_{\mathrm{ci}})^2} \tag{9}$$

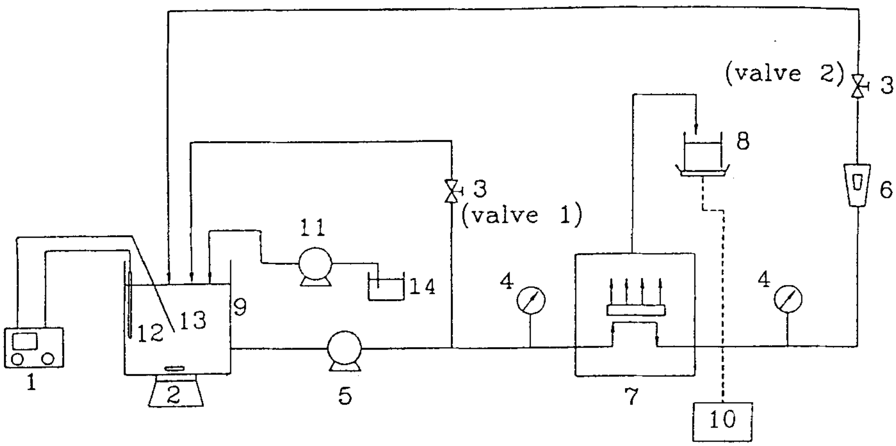

1. temp controller
2. stirrer
3. valves
4. pressure gauge
5. squeezing pump
6.rotameter
7. filtration cell
8. electronic balance
9. stock tank
10. recorder
11. micro-metering pump
12. heater
13. temp sensor
14. deionized water beaker

FIG. 2 Schematic diagram of experimental set-up (10).

$$u_{bni} = \frac{KT}{3\pi\mu d_{pn}(h - \sum h_{ci})} \tag{10}$$

$$C_{ni} = C_n - \frac{\sum W_{ni}}{\rho_p V_t} \tag{11}$$

A stepwise iterative procedure is then used to calculate the unsteady-state permeate flux from Eqs. (3) and (8)–(11).

EXPERIMENTAL APPARATUS AND METHODS

The schematic diagram of the experimental setup is shown in Fig. 2 (10). The experimental apparatus and method employed in this study were similar to those used by Chang and Hwang (10) except that polydispersed suspensions were substituted for monodispersed suspensions. The diameters and density of the polystyrene latex particles used in the suspensions were 0.303, 0.606, and 1.020 μm, and 1.05 g/cm^3, respectively. The volume of each particle size varied among the polydispersed suspensions, but the total volume concentration was always kept at 50 ppmv. It should be noted that for all experimental runs, the diameters of the suspension particles were always much larger than the membrane pore size to prevent particle penetration into or through the membrane.

RESULTS AND DISCUSSION

Determination of the Specific Resistance (α) and Voidage (ϵ_c) of the Cake

For constant pressure dead-end microfiltration, the specific resistance, α, can be obtained from the slope of the linear plot t/V vs V using the following filtration equation:

$$\frac{t}{V} = \frac{\mu R_m}{\Delta P A_m} + \alpha \left[\frac{\mu \rho_p C}{2\Delta P A_m^2}\right] V \tag{12}$$

For microfiltration of a polydispersed suspension, the particle size distribution, and hence the mean particle size in the suspension and the cake varied with time due to different magnitude of the forces acting on various sizes of the particles in the suspension. Figures 3–6 show the variation of the mean particle size of the instantaneous cake with time according to our proposed model. As a result, the specific resistance of the cake also varied with time. The variation of the specific resistance of the cake during microfiltration could be obtained from dead-end microfiltration ex-

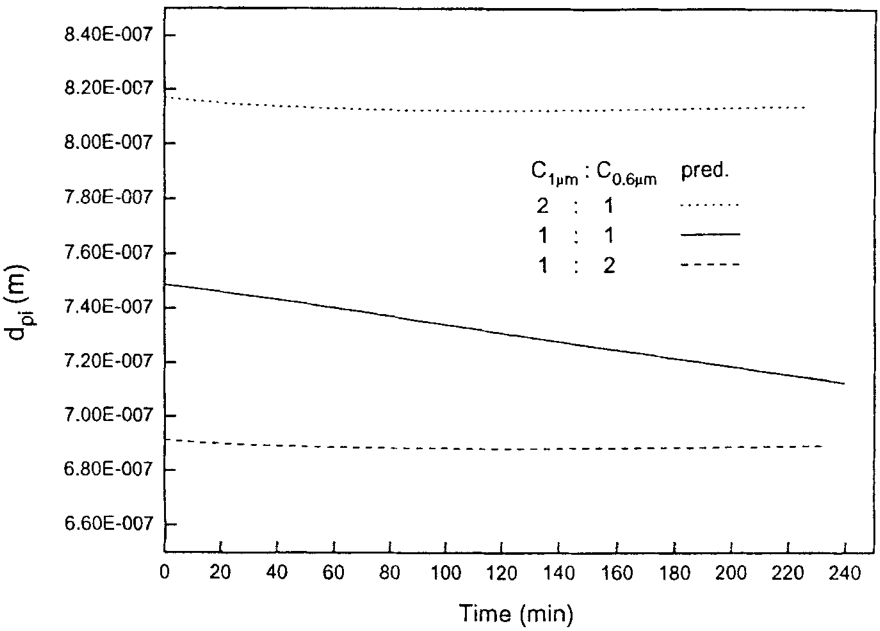

FIG. 3 The mean particle size of the instantaneous cake vs time (d_p = 1 + 0.6 μm).

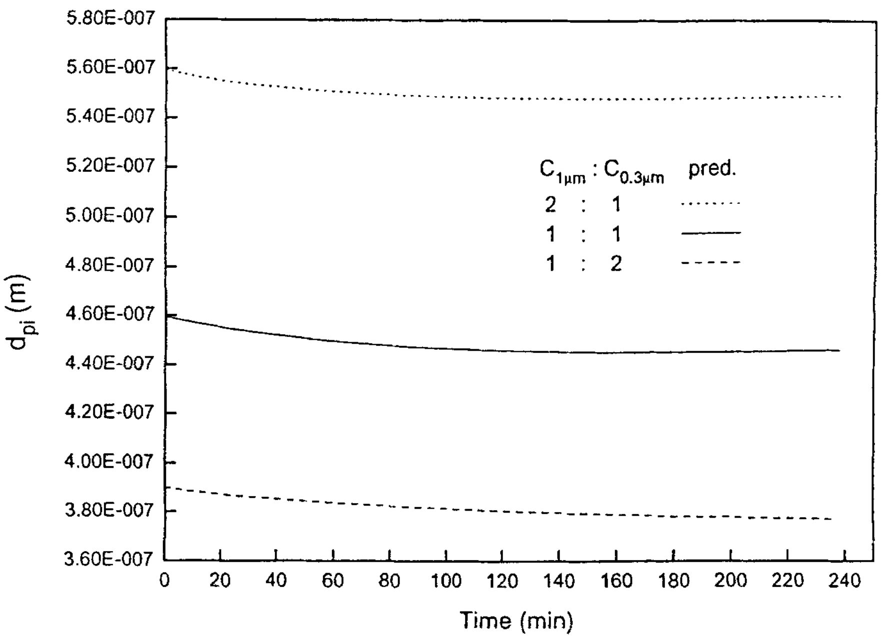

FIG. 4 The mean particle size of the instantaneous cake vs time (d_p = 1 + 0.3 μm).

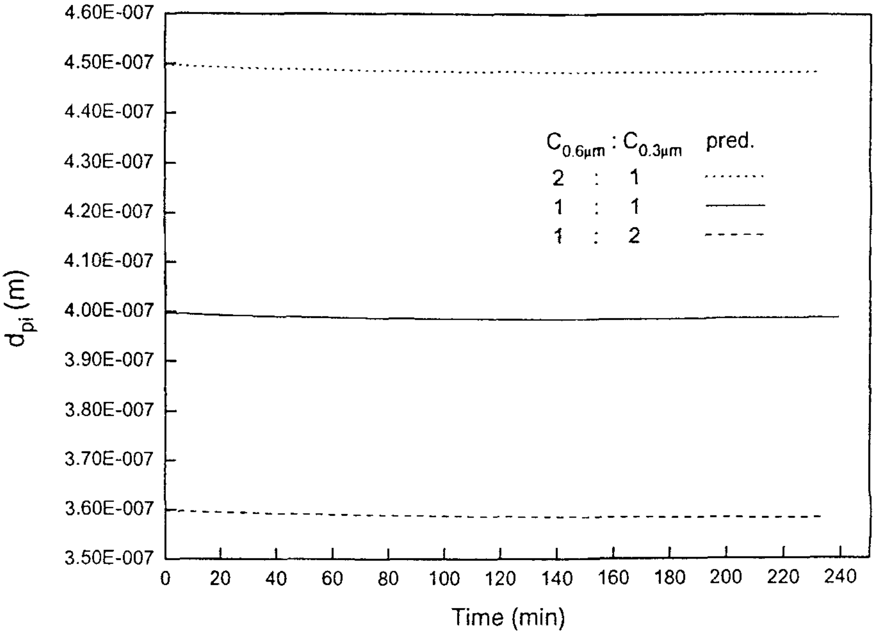

FIG. 5 The mean particle size of the instantaneous cake vs time (d_p = 0.6 + 0.3 μm).

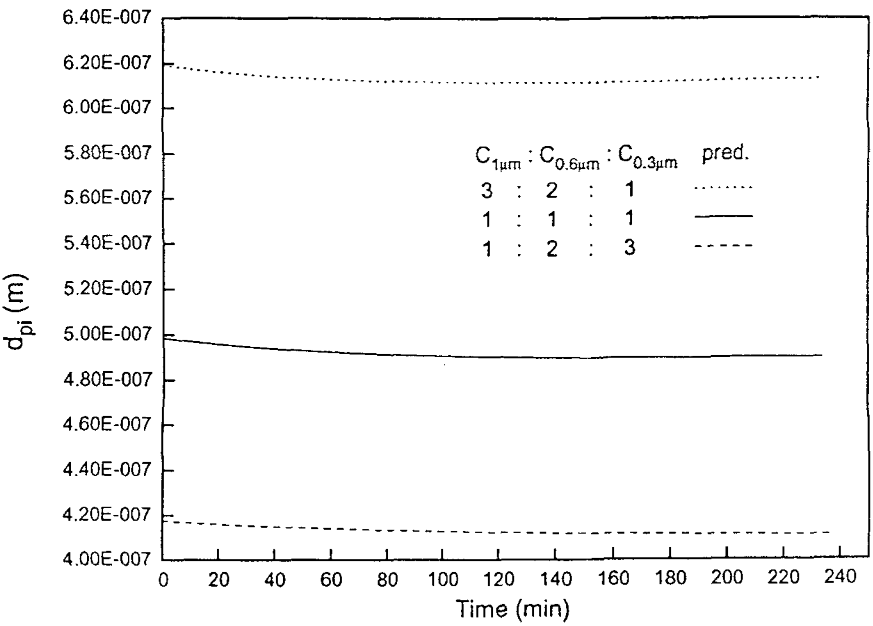

FIG. 6 The mean particle size of the instantaneous cake vs time (d_p = 1 + 0.6 + 0.3 μm).

periments using polydispersed suspensions with various volumes of each particle. The voidage of the cake, ϵ_c, could then be evaluated by the Carman–Kozeny equation:

$$\alpha = \frac{180(1 - \epsilon_c)}{\epsilon_c^3 \rho_p d_{pa}^2} \tag{13}$$

The relationships between the voidage and mean particle size of the cake obtained from the dead-end experiments for various polydispersed suspensions are shown in Figs. 7–10. As expected, the voidage of the cake increases with an increase in the mean particle size of the cake. In addition, the relationship between ϵ_c and d_{pa} can be described by the following correlation equation:

$$\epsilon_c = A_0 + A_1 d_{pa} + A_2 d_{pa}^2 \tag{14}$$

The values of the coefficients for various polydispersed suspensions are shown in Table 1. Note that the voidage of the cake obtained from the dead-end experiments is applicable to crossflow microfiltration.

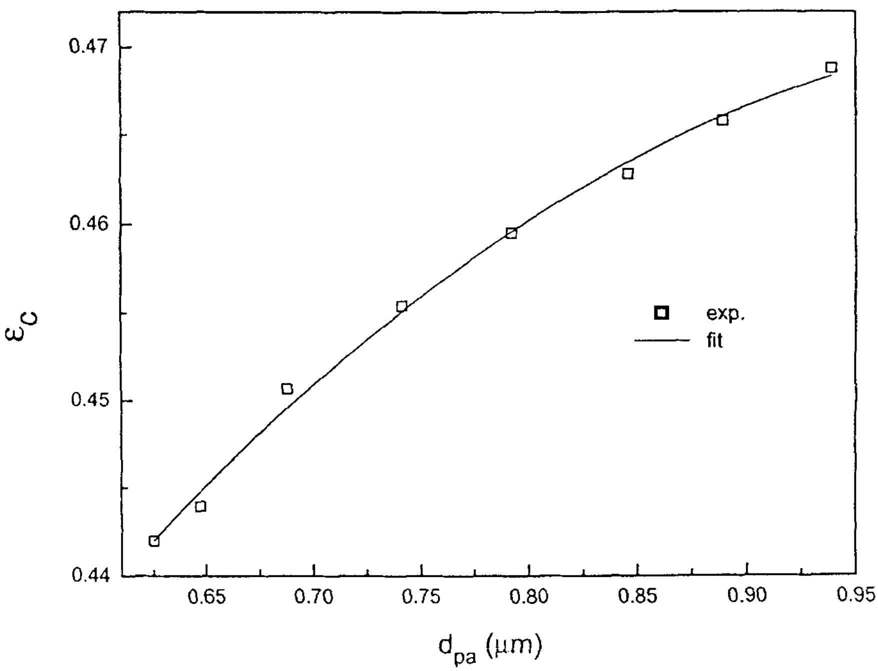

FIG. 7 The relationship between the voidage and mean particle size of the cake (d_p = 1 + 0.6 μm).

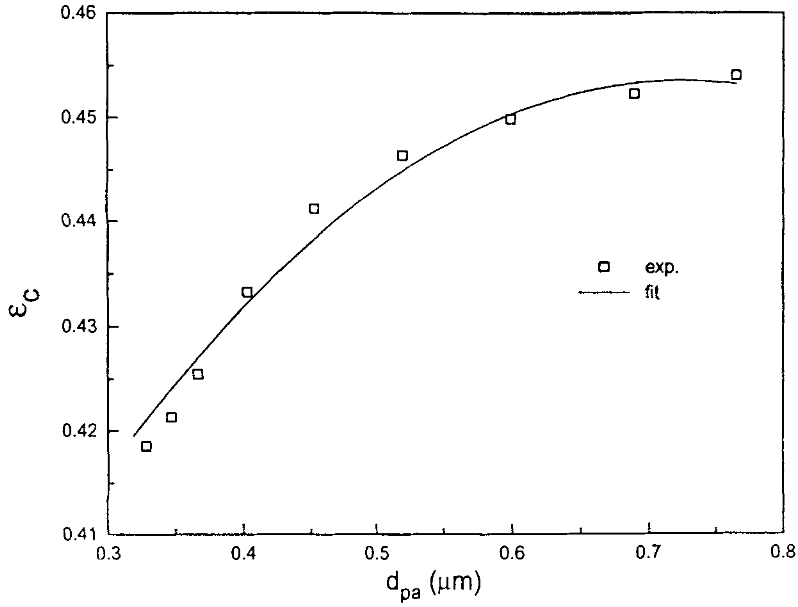

FIG. 8 The relationship between the voidage and mean particle size of the cake (d_p = 1 + 0.3 μm).

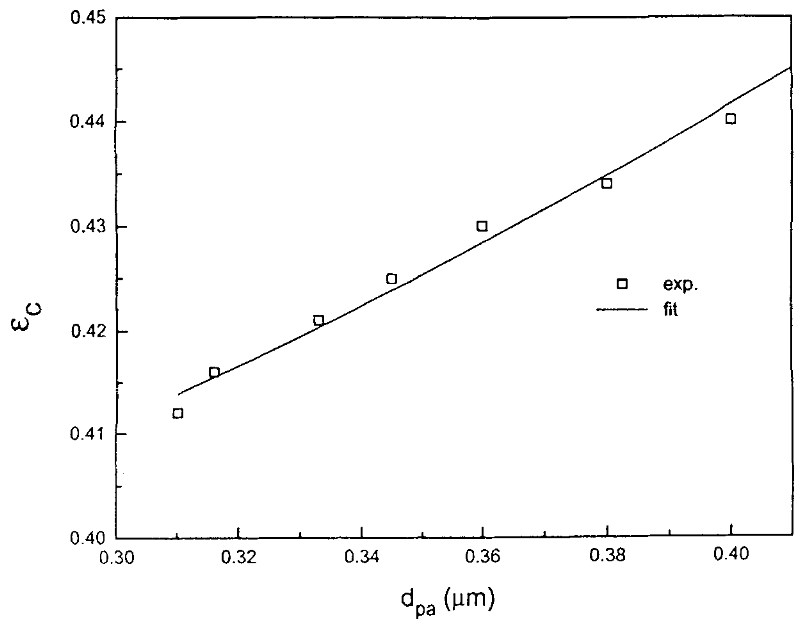

FIG. 9 The relationship between the voidage and mean particle size of the cake (d_p = 0.6 + 0.3 μm).

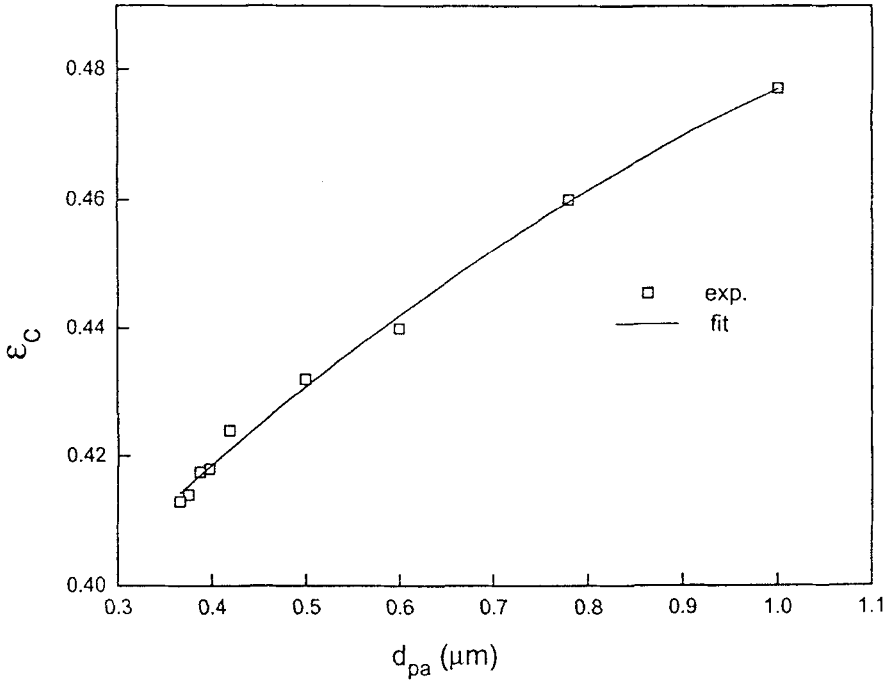

FIG. 10 The relationship between the voidage and mean particle size of the cake (d_p = 1 + 0.6 + 0.3 μm).

Unsteady-State Permeate Flux

The effects of particle size distribution on the unsteady-state permeate flux are shown in Figs. 11–14. It is seen in these figures and Figs. 3–6 that the unsteady-state permeate flux increases with an increase in the mean particle size of the cake. This is due to the fact that the voidage of

TABLE 1
The Parameter Values of the Correlation Equations
($\epsilon_c = A_0 + A_1 d_{pa} + A_2 d_{pa}^2$)

d_p (μm)	A_0	A_1	A_2
1 + 0.6	0.305	0.310	−0.145
1 + 0.3	0.327	0.366	−0.264
0.6 + 0.3	0.368	0.027	0.394
1 + 0.6 + 0.3	0.360	0.166	−0.050

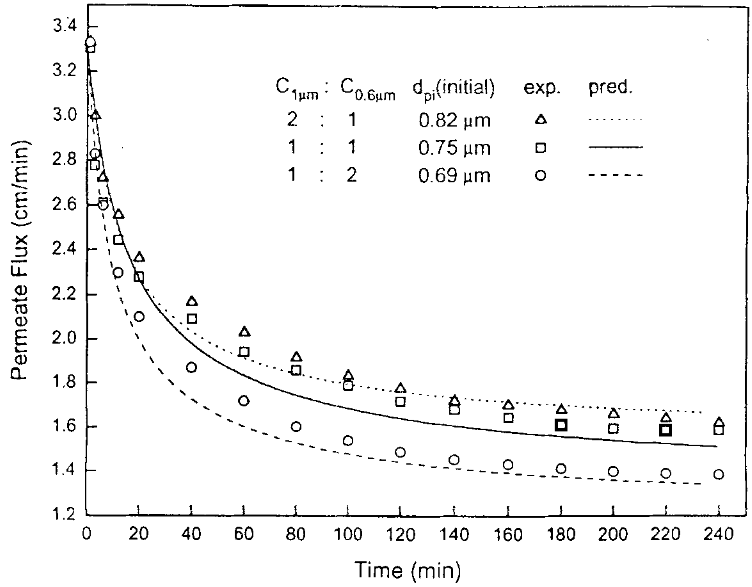

FIG. 11 Effect of particle size distribution on the permeate flux (d_m = 0.1 μm, ΔP = 3.8 × 10^4 Nt/m^2, T = 30°C, pH 6.6, u_o = 1.8 m/s, d_p = 1 + 0.6 μm).

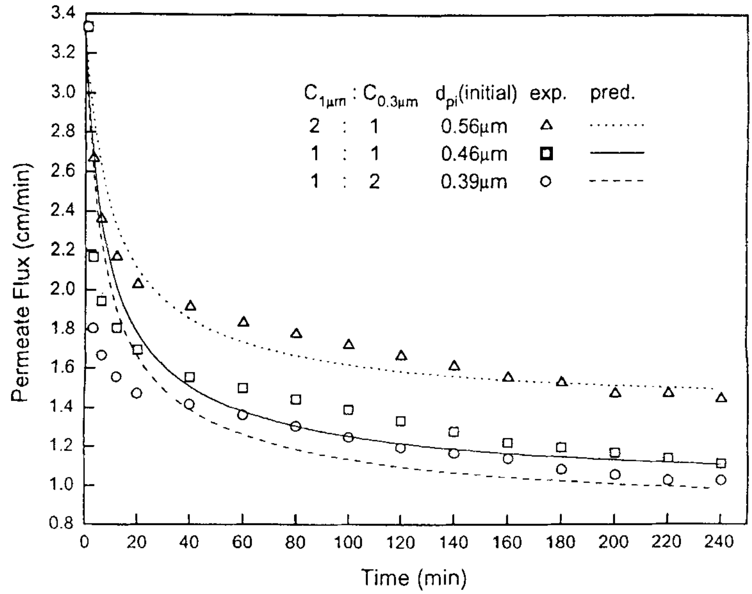

FIG. 12 Effect of particle size distribution on the permeate flux (d_m = 0.1 μm, ΔP = 3.8 × 10^4 Nt/m^2, T = 30°C, pH 6.6, u_o = 1.8 m/s, d_p = 1 + 0.3 μm).

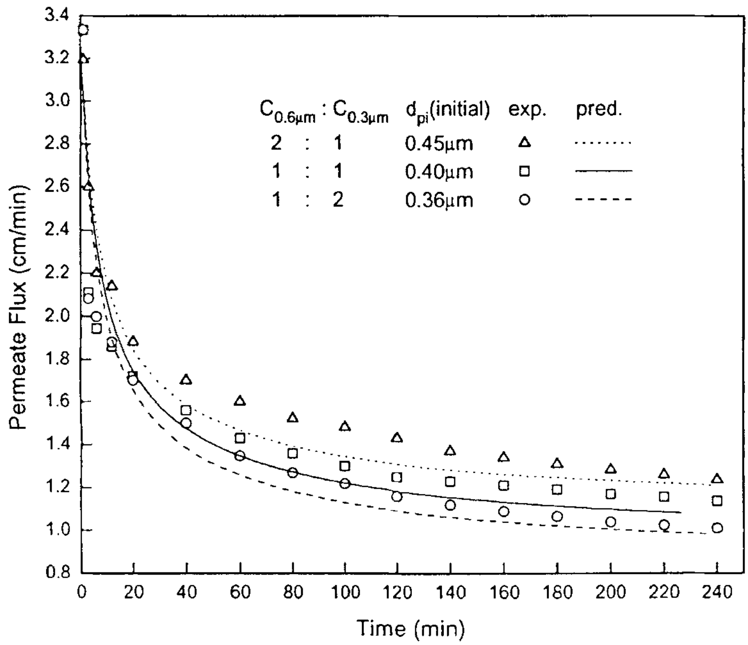

FIG. 13 Effect of particle size distribution on the permeate flux (d_m = 0.1 μm, ΔP = 3.8 × 10^4 Nt/m^2, T = 30°C, pH 6.6, u_o = 1.8 m/s, d_p = 0.6 + 0.3 μm).

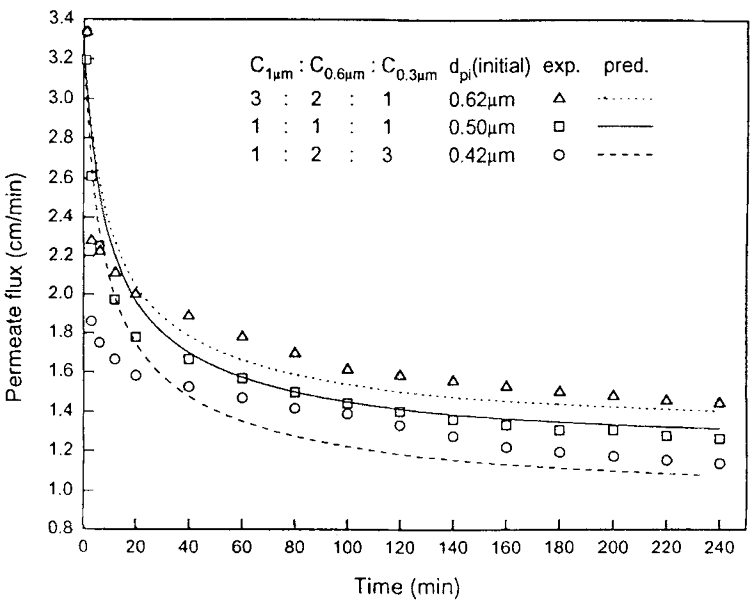

FIG. 14 Effect of particle size distribution on the permeate flux (d_m = 0.1 μm, ΔP = 3.8 × 10^4 Nt/m^2, T = 30°C, pH 6.6, u_o = 1.8 m/s, d_p = 1 + 0.6 + 0.3 μm).

the cake increases as the mean particle size of the cake is increased, which leads to a lower cake resistance. As a result, the unsteady-state permeate flux is higher for a higher mean particle size of the cake. It should be noted that the mean particle size of the cake increases as the mean particle size of the polydispersed suspension is increased. Therefore, the unsteady-state permeate flux increases with increasing mean particle size of the polydispersed suspension. Also shown in Figs. 7–10 is that the model predictions are in agreement with the experimental results.

CONCLUSIONS

Experiments were conducted to study crossflow microfiltration of polydispersed suspensions of spherical polystyrene latex particles. It was found that the unsteady-state permeate flux and the voidage of the cake increased with increasing mean particle size of the polydispersed suspension. A mathematical model based on a hydrodynamic theory and mass balance was also developed in this study. This model could satisfactorily predict the unsteady-state permeate flux of crossflow microfiltration of polydispersed suspensions.

NOTATIONS

A	Hamaker constant (J)
A_b	cross-section area of channel (m^2)
A_m	filtration area of membrane (m^2)
C_1	concentration of particle size 1 in the suspension (ppmv)
C_2	concentration of particle size 2 in the suspension (ppmv)
C_n	concentration of particle size n in the suspension (ppmv)
C_{1i}	concentration of particle size 1 in the suspension at time t (ppmv)
C_{2i}	concentration of particle size 2 in the suspension at time t (ppmv)
C_{ni}	concentration of particle size n in the suspension at time t (ppmv)
d_p	particle diameter (m)
d_{pa}	mean particle size of the cake in dead-end microfiltration (m)
d_{pi}	mean particle size of the instantaneous cake at time t (m)
d_{p1}	diameter of particle size 1 (m)
d_{p2}	diameter of particle size 2 (m)
d_{pn}	diameter of particle size n (m)
h	clearance of crossflow channel (m)
h_{ci}	thickness of the instantaneous cake at time t (m)
K	Boltzmann constant (J/K)
N_i	number of particles
ΔP	pressure drop across membrane (Nt/m^2)
R_c	cake resistance (1/m)
R_{ci}	the resistance of the instantaneous cake at time t (1/m)

R_m membrane resistance (1/m)
T temperature (K)
t filtration time (min)
u_{bni} modified Brownian diffusion for particle size n (m/s)
u_{lni} modified lateral lift velocity for particle size n (m/s)
u_o crossflow velocity (m/s)
u_{oi} modified u_o (m/s)
u_p permeate flux (m/s)
u_{sni} modified shear-induced velocity for particle size n (m/s)
u_{t1} backtransport velocity of particle size 1 (m/s)
u_{t2} backtransport velocity of particle size 2 (m/s)
u_{tn} backtransport velocity of particle size n (m/s)
u_x axial velocity of particle (m/s)
V cumulative volume of the permeate (m^3)
V_t volume of the suspension in stock tank (m^3)
W_{1i} weight of particle size 1 of the instantaneous cake at time t (kg)
W_{2i} weight of particle size 2 of the instantaneous cake at time t (kg)
W_{ni} weight of particle size n of the instantaneous cake at time t (kg)
X_d Debye length (m)

Greek Letters

α specific resistance of cake (m/kg)
α_i specific resistance of the instantaneous cake at time t (m/kg)
μ viscosity of the suspension (kg/ms)
ϵ_o dielectric constant of the suspension (Nt/V^2)
ϵ_c cake voidage
ϵ_{ci} cake voidage of the instantaneous cake at time t
ζ zeta potential (V)
ρ water density (kg/m^3)
ρ_p particle density (kg/m^3)
ρ_{p1} density of particle size 1 (kg/m^3)
ρ_{p2} density of particle size 2 (kg/m^3)
ρ_{pn} density of particle size n (kg/m^3)

REFERENCES

1. R. D. Cohen and R. F. Probstein, "Colloidal Fouling of Reverse Osmosis Membrane," *J. Colloid Interface Sci.*, *114*, 194 (1986).
2. G. Green and G. Belfort, "Fouling of Ultrafiltration Membrane: Lateral Migration and Particle Trajectory Model," *Desalination*, *35*, 129 (1980).
3. M. R. Wiesner, M. M. Clark, and J. Mallevialle, "Membrane Filtration of Coagulated Suspensions," *J. Environ. Eng.*, *115*, 20 (1989).

4. J. W. Hunt, C. J. Brouckaert, K. Treffry-Goatley, and C. A. Buckley, "The Unsteady-State Modeling of Crossflow Microfiltration," *Desalination*, *64*, 443 (1987).
5. H. B. Dharmappa, J. Verink, R. Ben Aim, K. Yamamoto, and S. Vigneswaran, "A Comprehensive Model for Crossflow Filtration Incorporating Polydispersity of Influent," *J. Membr. Sci.*, *65*, 173 (1992).
6. R. T. Davis and S. A. Birdshell, "Hydrodynamic Model and Experiments for Crossflow Microfiltration," *Chem. Eng. Commun.*, *49*, 217 (1987).
7. C. A. Romero and R. H. Davis, "Experimental Verification of the Shear-Induced Hydrodynamic Diffusion Model of Crossflow Microfiltration," *J. Membr. Sci.*, *62*, 249 (1991).
8. N. J. Blake, I. W. Cumming, and M. Streat, "Prediction of Steady Crossflow Filtration Using a Force Balance Model," *Ibid.*, *68*, 205 (1992).
9. V. L. Pillary and C. A. Buckley, "Cake Formation in Crossflow Microfiltration Systems," *Water Sci. Technol.*, *24*(10), 149 (1992).
10. D. J. Chang and S. J. Hwang, "Unsteady-State Permeate Flux of Crossflow Microfiltration," *Sep. Sci. Technol.*, *29*(12), 1593 (1994).

Received by editor December 13, 1994